

# Corneous $\beta$ -proteins

Subjects: Biology

Contributor: David Parry

The epidermal appendages of birds and reptiles (the sauropsids) include claws, scales, and feathers. Each has specialized physical properties that facilitate movement, thermal insulation, defence mechanisms, and/or the catching of prey. The mechanical attributes of each of these appendages originate from its fibril-matrix texture, where the two filamentous structures present, i.e., the corneous  $\beta$ -proteins (CBP or  $\beta$ -keratins) that form 3.4 nm diameter filaments and the  $\alpha$ -fibrous molecules that form the 7–10 nm diameter keratin intermediate filaments (KIF), provide much of the required tensile properties. The matrix, which is composed of the terminal domains of the KIF molecules and the proteins of the epidermal differentiation complex (EDC) (and which include the terminal domains of the CBP), provides the appendages, with their ability to resist compression and torsion.

Keywords: corneous  $\beta$ -proteins ; keratin intermediate filaments ; X-ray fiber diffraction

---

## 1. Introduction

Many techniques have been employed in an effort to gain a deeper understanding of the structures of the constituent CBP molecules, their assembly into filaments and the lateral assembly of those filaments with respect to one another. Such techniques include electron microscopy, fiber X-ray diffraction, infrared spectroscopy, protein chemistry, sequences analyses, and model building. The 3.4 nm diameter filaments are a major constituent of all of the epidermal appendages present in the sauropsids and, as such, it is important to understand their detailed structures if we are to understand their mechanical attributes. It is noted, of course, that although these filaments are but one component in the tissue as a whole, their contribution is clearly a major one and well worthy of detailed study.

## 2. Structure of the Corneous $\beta$ -Protein Molecules and Their Assembly into Filaments

Early X-ray diffraction patterns using specimens of well-orientated feather rachis revealed a highly regular structure that was believed to originate from the filamentous component of the rachis . Since this was generally similar to the pattern obtained from stretched  $\alpha$ -keratin, it was suggested that the conformation of the molecules in the 3.4 nm diameter filaments of avian and reptilian keratins was based on the  $\beta$ -sheet conformation, rather than that of the  $\alpha$ -helix <sup>[1]</sup>. More detailed research showed that the filaments consisted of a helical arrangement of small  $\beta$ -crystallites with four-fold screw symmetry <sup>[2][3][4]</sup>. The pitch length ( $P$ ) of the helix in feather keratin was 9.6 nm and the axial rise ( $h$ ) per repeating unit was 2.4 nm. Small changes in  $P$  have been observed in some tissues (9.2 nm in chicken scale <sup>[5]</sup>; 9.28 nm in snake scale <sup>[6]</sup>; 9.85 nm in lizard claw <sup>[6]</sup>) but the four-fold screw symmetry is maintained. It would seem probable, therefore, that the basic helical framework of the filaments is conserved across all of the sauropsids.

The first sequence determined for any CBP was that from emu feather <sup>[7]</sup>. One enzymatically-derived fragment was shown by infrared spectroscopy to have a high  $\beta$ -sheet content with the chain looped back and forth in an antiparallel conformation <sup>[8][9]</sup>. A subsequent analysis of the whole sequence revealed that the  $\beta$ - and turn-favoring residues were confined to a central portion of the chain and that these residue groupings had out-of-phase periodicities of about eight residues <sup>[10]</sup> (Figure 1). The predicted length of the  $\beta$ -strands was thus about 2.4 nm, a value that corresponded precisely to the meridional repeat derived from the X-ray diffraction patterns. Sequence analyses by Sawyer et al. <sup>[11]</sup> recognized the high degree of homology across the avian CBPs and also noted that a 20 residue segment existed in the bird sequences that was homologous to that in alligator claw. This same region was seen in the archosaurs and squamates <sup>[12]</sup> and it was, therefore, suggested <sup>[13]</sup> that this region played a role in assembly. A sequence homologous to that recognized earlier in emu feather with the postulated  $\beta$ -conformation was subsequently observed in a reptilian claw <sup>[14][15]</sup>, and since that time it has been shown that a  $\beta$ -containing central domain 34-residue long that encompasses the former 20 residue region is highly conserved in the CBPs across all species and appendages <sup>[16][17][18][19]</sup>. Immediately N- and C-terminal to the 34-residue sequence there are short pieces of sequence about 7–11 residues long that are also largely conserved

and it has been speculated that 142 these are likely to be involved in some way in filament assembly [16]. From model building, it can be deduced that the  $\beta$ -crystallites will form the framework of the filaments. Using the quantitative fit to the X-ray diffraction patterns as a criterion for the model building it was further shown that the crystallites must be formed from a pair of antiparallel  $\beta$ -sheets—a  $\beta$ -sandwich [20][21]—and that these sheets will be related to one another by a perpendicular dyad axis of rotation. Further, the X-ray data demanded that the sheets could not be planar but must be twisted in what is now believed to be a right-handed manner [22].

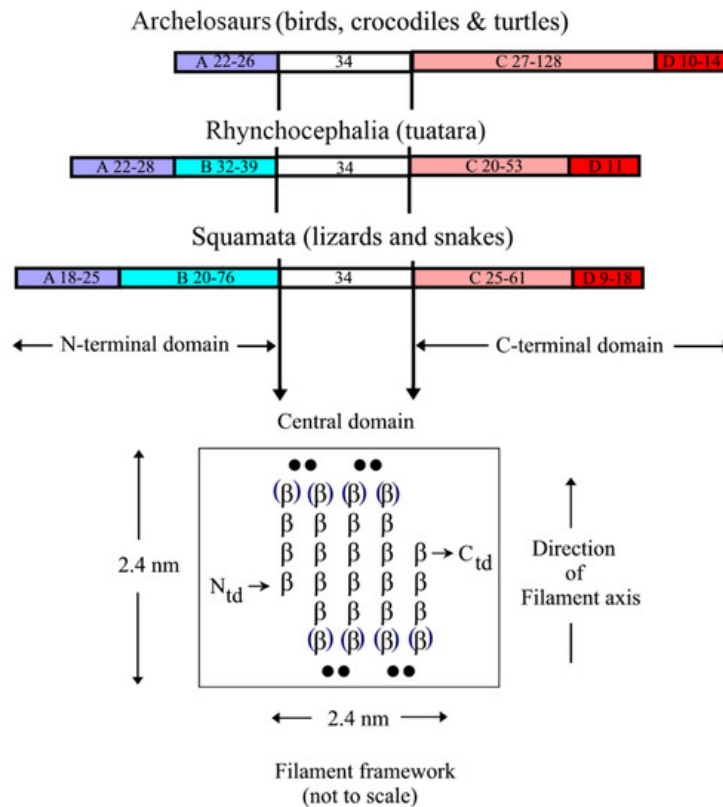


**Figure 1.** Sequence comparisons of the CBPs from the sauropsids reveal that the N-terminal domain is comprised of subdomain A in the archelosaurs, but subdomains A and B in the squamates and rhynchocephalia. The C-terminal domain, however, comprises subdomains C and D in all of the sauropsids. The sequence characteristics of each subdomain are listed in the text. The approximate size ranges of the subdomains are listed. The central 34-residue domain adopts a twisted  $\beta$ -sheet structure with three inner strands and two partial outer ones that assemble in an antiparallel manner with a similar sheet from a different chain to form a  $\beta$ -sandwich. In turn, these assemble axially with a four-fold screw symmetry to form a filamentous structure of diameter 3.4 nm. Figure reproduced from [19] with permission of Springer.

A number of other, key observations provided support for these conclusions. Firstly, one face of the  $\beta$ -sheet in the 34-residue repeat was shown to be largely composed of apolar residues (amphipathic), thereby providing a ready and simple means by which a pair of these sheets could assemble via their apolar faces to form a  $\beta$ -sandwich [23]. The amphipathic nature of one face of the  $\beta$ -sheet was independently confirmed [24] using a molecular mechanics and Poisson Boltzmann approach. Secondly, the sequences of the central turns 2 and 3 in the  $\beta$ -crystallites (consensus sequences Q/R-P-P/S-P and L/I-P-G-P, respectively) were strongly conserved across all chains implying that the axial assembly of the  $\beta$ -crystallites will be dependent on the strong apolar interactions that these residues would provide (Figure 2; [16][18][24]).

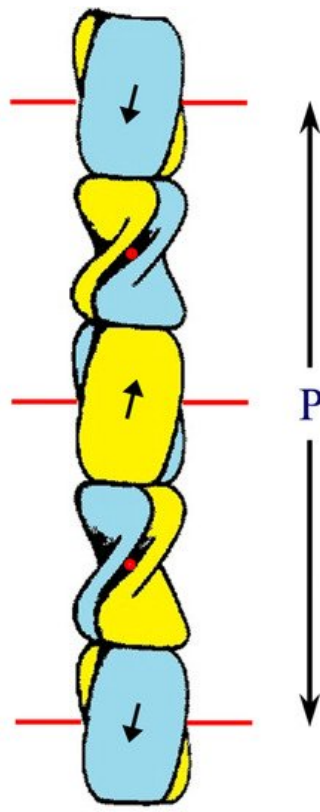


**Figure 2.** Schematic diagram of the  $\beta$ -sandwich formed from the conserved 34-residue stretch of sequence in each of two CBP chains. Each sandwich is comprised of a pair of right-handed twisted antiparallel  $\beta$ -sheets (one is drawn blue and the other is yellow) and these are related to one another by a perpendicular dyad axis of rotation (marked alternatively by red circles and red lines). Axial assembly of the  $\beta$ -sandwiches through the application of a left-handed four-fold screw axis generates a 3.4 nm diameter filament of pitch length 9.6 nm and axial rise 2.4 nm. Figure reproduced from [19] with permission of Springer.

Modeling of the  $\beta$ -sandwich with a perpendicular dyad axis relating the two constituent  $\beta$ -sheets indicates that the latter will contain three central  $\beta$ -strands and two partial outer ones. This, naturally, leads to close packing between the sheets of the residues in the inner strands and occurs in layers perpendicular to the fiber axis [18]. In an alternative model [24], each  $\beta$ -sheet would contain four central  $\beta$ -strands and the two sheets would be related to one another by a parallel dyad axis of rotation. However, close packing of residues between the sheets would be compromised and, furthermore, parts of the X-ray diffraction pattern (even layer lines in the 0.3 nm region and odd layer lines in the 0.6 nm region) would be less compatible with such a model [22][25].

The terminal domains of the CBP, i.e., those sequences immediately N- and C-terminal to the conserved 34-residue region show considerable substructure but one that differs between the archelosaurs and the lepidosaurs (Figure 1; [17]). In the former case (birds, crocodiles, and turtles), the N-terminal domain is comprised of a single domain (subdomain A), whereas in the latter (tuatara, snakes, and lizards) there are two subdomains, A and B. Subdomain A is typically about 25 residue long and is cysteine- and proline-rich, and subdomain B is variable in length (20–76 residues) and contains multiple sequence repeats based on glycine, serine, alanine, leucine, and the aromatic residues. In tuatara, three types of N-terminal domains have been recognized but with this exception the pattern discussed above is maintained [26]. The C-terminal domain of all the sauropsids comprises two subdomains, C and D. Subdomain C, like subdomain B, is variable in length (20–128 residues) but, unlike subdomain B, is essentially rich in just glycine and tyrosine residues, often in repeating sequences. Subdomain D is short (9–18 residues), cysteine-, arginine- and lysine-rich, and occurs at the C-terminal end of the chain. It will be indicated in Section 2.3 that the terminal domains are important in specifying the physical attributes of the epidermal appendages and that an appropriate mix of family members might have the capability of fine-tuning these properties.

## References

1. Astbury, W.T.; Marwick, T.C. X-ray interpretation of the molecular structure of feather keratin. *Nature* 1932, 130, 309–310.
2. Fraser, R.D.B.; MacRae, T.P. Molecular organization in feather keratin. *J. Mol. Biol.* 1959, 1, 387–397.

3. Fraser, R.D.B.; MacRae, T.P. Structural organization in feather keratin. *J. Mol. Biol.* 1963, 7, 272–280.
4. Schorr, R.; Krimm, S. Studies on the structure of feather keratin I. X-ray diffraction studies and other experimental data. *Biophys. J.* 1961, 1, 467–487.
5. Stewart, M. The structure of chicken scale keratin. *J. Ultrastruct. Res.* 1977, 60, 27–33.
6. Rudall, K.M. X-ray studies of the distribution of protein chain types in the vertebrate epidermis. *Biochim. Biophys. Acta* 1947, 1, 549–562.
7. O'Donnell, I.J. The complete amino acid sequence of a feather keratin from emu (*Dromaius novae-hollandiae*). *Aust. J. Biol. Sci.* 1973, 26, 415–437.
8. Fraser, R.D.B.; Suzuki, E. Polypeptide chain conformation in feather keratin. *J. Mol. Biol.* 1965, 14, 279–282.
9. Suzuki, E. Localization of beta-conformation in feather keratin. *Aust. J. Biol. Sci.* 1973, 26, 435–437.
10. Fraser, R.D.B.; MacRae, T.P. The molecular structure of feather keratin. In *Proceedings of the 16th International Ornithological Congress, Canberra, Australia, 12–17 August 1976*; pp. 443–451.
11. Sawyer, R.H.; Glenn, T.; French, J.O.; Mays, B.; Shames, R.B.; Barnes, G.L.; Rhodes, W.; Ishikawa, Y. The expression of beta ( $\beta$ ) keratins in the epidermal appendages of reptiles and birds. *Am. Zool.* 2000, 40, 530–539.
12. Alibardi, L.; Toni, M.  $\beta$ -keratins of reptilian scales share a central amino acid sequence termed core-box. *Res. J. Biol. Sci.* 2007, 2, 329–339.
13. Dalla Valle, L.; Nardi, G.B.; Bonazza, G.; Zuccal, C.; Emera, D.; Alibardi, L. Forty keratin-associated  $\beta$ -proteins ( $\beta$ -proteins) form the hard layers of scales, claws, adhesive pads in the green anole lizard, *Anolis carolinensis*. *J. Exp. Zool. Part B Mol. Dev. Evol.* 2010, 314B, 11–32.
14. Inglis, A.S.; Gillespie, M.J.; Roxborough, C.M.; Whitaker, L.A.; Casagrande, F. Sequence of a glycine-rich protein from lizard claw: Unusual dilute acid and heptafluorobutyric acid cleavages. In *Proteins, Structure and Function*; L'Italien, J.L., Ed.; Plenum: New York, NT, USA, 1987; pp. 757–764.
15. Fraser, R.D.B.; Parry, D.A.D. The molecular structure of reptilian keratin. *Int. J. Biol. Macromol.* 1996, 19, 207–211.
16. Fraser, R.D.B.; Parry, D.A.D. Amino acid sequence homologies in the hard keratins of birds and reptiles, and their implications for molecular structure and physical properties. *J. Struct. Biol.* 2014, 188, 213–224.
17. Fraser, R.D.B.; Parry, D.A.D. The structural basis of the filament-matrix texture in the avian/reptilian group of hard  $\beta$ -keratins. *J. Struct. Biol.* 2011, 173, 391–405.
18. Fraser, R.D.B.; Parry, D.A.D. Molecular packing in the feather keratin filament. *J. Struct. Biol.* 2008, 162, 1–13.
19. Fraser, R.D.B.; Parry, D.A.D. Filamentous structure of hard  $\beta$ -keratin in the epidermal appendages of birds and reptiles. In *Subcellular Biochemistry: Fibrous Proteins: Structures and Mechanisms*; Parry, D.A.D., Squire, J.M., Eds.; Springer: Cham, Switzerland, 2017; Volume 82, pp. 231–252.
20. Chothia, C.; Finkelstein, A.V. The classification and origins of protein folding patterns. *Ann. Rev. Biochem.* 1990, 57, 107–1039.
21. Kister, A.E.; Finkelstein, A.V.; Gelfand, I.M. Common features in structures and sequences of sandwich-like proteins. *Proc. Natl. Acad. Sci. USA* 2002, 99, 14137–14141.
22. Fraser, R.D.B.; MacRae, T.P.; Parry, D.A.D.; Suzuki, E. The structure of feather keratin. *Polymer* 1971, 12, 35–56.
23. Hallahan, D.L.; Keiper-Hrynko, N.M.; Shang, T.Q.; Ganzke, T.S.; Toni, M.; Dalla Valle, L.; Alibardi, L. Analysis of gene expression in gecko digital adhesive pads indicates significant production of cysteine- and glycine-rich beta keratins. *J. Exp. Zool.* 2009, 312B, 58–73.
24. Calvaresi, M.; Eckhart, L.; Alibardi, L. The molecular organization of the beta-sheet region in corneous beta-proteins (beta-keratins) of sauropsids explains its stability and polymerization into filaments. *J. Struct. Biol.* 2016, 194, 282–291.
25. Fraser, R.D.B.; Parry, D.A.D. Lepidosaur  $\beta$ -keratin chains with four 34-residue repeats: Modelling reveals a potential filament-crosslinking role. *J. Struct. Biol.* 2020, 209, 107413.
26. Holthaus, K.B.; Alibardi, L.; Tschachler, E.; Eckhart, L. Identification of epidermal differentiation genes of the tuatara provides insights into the early evolution of lepidosaurian skin. *Sci. Rep.* 2020, 20, 12844.